A Deep Learning Framework for Personalized Brain Metastasis Prognosis and Diagnosis

Deepinder Kaur[1], Jaspreet Singh[2]

[1,2]Chandigarh University, Mohali, Punjab, India
Email: deepinder.research9237@gmail.com[1], jaspreet.e10279@cumail.in[2]

Received: 10.07.2024 Revised: 14.08.2024 Accepted: 25.09.2024

ABSTRACT
Brain Metastasis present important diagnostic and therapeutic problems, occurring in from 10% to 30% of cancer patients, significantly affecting cognitive function. Manual interpretation of MRI is a routine but time-consuming task that may be imprecise in the case of tiny or diverse tumors. This paper presents a novel approach for automatic brain metastasis segmentation on MRI data using a U-Net model. This method fuses several imaging modalities to refine the identification of BM. These include T1-weighted, T2-weighted, T1 contrast enhanced, and FLAIR. The dataset used for this purpose is the University of California San Francisco Brain Metastases Stereotactic Radiosurgery (UCSF-BMSR) MRI dataset. The model was trained, tested, and verified using this dataset. The U-Net model with dropout performed quite well with an overall accuracy of 99.75%; Dice, 64.49%; and IOU, 96.81%. In this paper, the proposed method is compared to two baseline models: Convolutional Neural Networks and Fully Convolutional Networks. The U-Net outperformed the baselines on all the important measures and demonstrated great potential for being applied clinically in real life. This finding puts a finger on the capability of greatly improved detection accuracy with the U-Net model, and thus, timely treatment decisions.

Keywords: Brain Metastasis, U-Net, Convolution Neural Networks, Fully Convolutional Networks, Segmentation, BM detection.

1. INTRODUCTION

Brain Metastasis is a very complicated process in which cancer cells migrate to the brain from a distant extracranial site and metastasize to various intracerebral areas leading to brain dysfunction [1], [2]. About 10-30% of cancer patients experience such metastases, although the number of cytologically identifiable primary sources that metastases develop in the lungs, the breasts, the kidneys, the colons, and melanoma in the skin [3], [4]. BM from primary brain tumours can disseminate through either circular or lymphatic spreading systems[5]. This metastatic spread to the brain presents a unique set of challenges compared with primary brain tumors in terms of impact on prognosis and treatment strategies. The issue is of a significance high enough for research as it affects and influences so much in patients' health and mortality. In most cases, the BM may cause cognitive deficits in the patients that lead to distress and might worsen their quality of life [6], [7].

Further, the common treatments of BM like radiation therapy and surgery may cause inflammation, damage to healthy brain tissues that might lead to overall cognitive impairment like problem in memory or attention [8], [9]. Thus, accurate and timely prediction of BM is very important to reduce neurocognitive effects. Therefore, early prediction of BM with maximal sensitivity is warranted, as a delay in such a prediction may add to the neurocognitive burden. The diagnosis of BM has never been easy due to the heterogeneity of the tumor shape or size, the limitation of imaging techniques, and the risk of biopsies; however, accurately detecting BM is essential for disease surveillance and response evaluation in health care practice. Traditional methods largely rely on well-documented manual interpretation, mainly by expert clinicians, of MRI data as means for diagnosing brain metastases. Radiologists seldom have this much detail quantified during MRI interpretation; hence the process is very time-consuming when it comes to the detection and segmentation of BMs [10], [11]. Moreover, MRI and CT scan interpretation face difficulty in detecting small lesions or differentiating primary tumor types [12]. However, with advancements in 3D imaging techniques and usage of imaging modalities such as T1 weighted, T2-weighted, T1-contrast enhanced and FLAIR (Fluid-Attenuated Inversion Recovery) have improved the detection and characterization of BM [13], [14], [15].

Over the past two decades, Artificial intelligence (AI) has played an increasingly important role in detecting and segmenting BM with machine learning (ML) and deep learning (DL) techniques [16], [17],

[18], [19]. In this regard, different modalities have been explored for the automatic detection and segmentation of intracranial metastases. Deep learning framework-based automated systems have shown great promise in detecting BMs with increased accuracy regarding treatment success. Deep learning techniques, especially CNN, have already proved to be very effective in most medical imaging applications for image segmentation and image classification tasks [20], [21], [22]. The current study is going to introduce a new approach for the segmentation of brain metastases in MRI using a U-Net model.

The primary objective of the study is to develop a deep learning-based U-Net model that can automatically classify brain metastases from MRI scans. Also, the presented model rigorously evaluates the performance of the approach by considering diversity in the dataset and comparing it with prior works with two baseline models i.e., CNN (Convolutional Neural Networks) and FCN (Fully Convolutional Networks). This comparison seeks to assess the model's effectiveness in real-world clinical applications, ultimately contributing to the enhancement of diagnostic tools and improving patient outcomes through timely and accurate decision-making.

The following section summarizes previous research and present methods in the field of automated brain metastasis classification using MRI data. The next section describes the methodology that includes the study of dataset, design, and implementation of the proposed U-Net model. Furthermore, the results section is presented which showcases the performance metrics and outcomes of the proposed approach. The discussion that includes a comparison of proposed model and baseline models has been presented. Finally, the conclusion summarizes the important findings, emphasizes the study's contributions, and proposes future research areas

2. LITERATURE

Diagnoses and prognosis of brain metastases have rapidly changed due to improvements in medical imaging and machine learning or deep learning techniques. The current review has taken into consideration some of the major studies that led to the current understanding and application of various in tackling brain metastases. Recent studies could be categorized into three parts: classification of glioblastoma and brain metastases, detection and segmentation of brain metastases, and specific detection of brain metastases using black blood imaging.

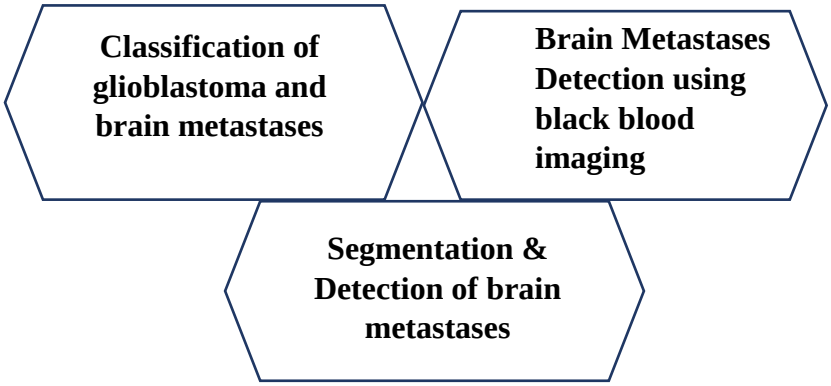

Fig 1. Literature Trio

2.1 Classification of glioblastoma and brain metastases

Accurate classification of glioblastoma (GB) and brain metastases (BM) poses a significant challenge due to their similar appearance on conventional MRI scans. Various machine learning approaches, including SVM and LASSO regression, deep neural networks, and CNNs, have been used to distinguish glioblastoma from brain metastases, with accuracy rates ranging from 69.2% to 90%. The table 1 below demonstrates key studies and their findings in this domain.

Table 1. Classification of glioblastoma and brain metastases

Objective	Reference	Methodology	Key Findings
Differentiate glioblastoma from brain metastases	[23]	SVM and LASSO regression on radiomic features	Achieved 90% accuracy in distinguishing GB from BM.
	[24]	SVC and MLP models on multimodal MRI	Achieved a maximum accuracy of 69.2% with the MLP model.

	[25]	Radiomics-based machine learning models, including DNN	Assessed the use of radiomics-based machine learning models, including DNN, for distinguishing GB from BM.
	[26]	Handcrafted radiomics (HCR) and deep learning-based radiomics (DLR)	Identified effective classifiers using HCR and HCR + DLR features on different MRI modalities.
	[27]	Metabolic Radiomics-based oxygen metabolism with deep convolutional neural networks (CNNs)	Outperformed human readers in all classification parameters for GB vs. BM.
	[28]	MRI analysis including FLAIR and ADC ratios	Differentiated mGBM from metastases using specific MRI criteria and ADC values, highlighting significant diagnostic differences.
	[29]	ResNet101 and VGG19 models	ResNet101 achieved 83% accuracy for MPBT, and VGG19 achieved 81% accuracy for MBT, demonstrating their effectiveness in classification.
	[30]	ML classifier and logistic regression with sphericity 3D radiomic index	ML classifier achieved balanced accuracy of 80% on test set; neuroradiologists had higher accuracy than residents and the classifier.

Research has shown high success rates in distinguishing glioblastoma from brain metastases, including subtypes like breast and lung metastases, using machine learning and deep learning algorithms.

2.2 Detection of brain metastases using black-blood imaging

In recent years, black blood imaging has emerged as a promising approach for detecting brain metastases, increasing the visibility of metastatic lesions by suppressing the signal from blood vessels and providing clearer delineation of abnormal features. Oh et al. [31] investigated brain metastasis identification using a You Only Look Once (YOLO) V2 network trained with 3D BB sampling perfection and application-optimized contrasts on various flip angle evolution images.

Table 2. BM Detection using black-blood imaging

Objective	Reference	Methodology	Key Findings
Detection of brain metastases using black blood imaging	[31]	Deep learning-based detection algorithm with contrast-enhanced BB imaging data	Showed high sensitivity in detecting BM, though with some false positives compared to other imaging methods.
	[21]	FDA-approved Artificial Intelligence (AI) segmentation software	Achieved significant efficiency gains (55.6% in PTVs, 75.8% in OARs) with need for human edits in certain structures.
	[32]	AI segmentation using Medical Mind software	Achieved an accuracy of 76.8% (86 out of 112) and a modified accuracy of 81.3% (91 out of 112) when considering targeted agents.
	[33]	Comparison of CNN performance using BB and CE T1 MRI sequences.	BB CNN: 92.3% accuracy, AUC 0.869; CE T1 CNN: 85.5% accuracy, AUC 0.534.

2.3 Detection and segmentation of brain metastases using ML and DL techniques

Recent research has revealed that applying machine learning (ML) and deep learning (DL) approaches to detect and segment brain metastases yields promising outcomes. Several ML and DL techniques, including SVM, Random Forest, CNN, U-Net architectures, have been assessed for their performance in segmenting brain tumours on MRI scans.

Table 3. BM Detection & Segmentation using ML/DL techniques

Objective	Reference	Methodology	Key Findings
Detection and segmentation of brain metastases using ML and DL techniques	[34]	3D-FCN (Fully Convolutional Network)	Emphasizes the importance of accurate and efficient segmentation for improving clinical outcomes and reducing manual effort. sensitivity was 0.96 ± 0.03, the specificity was 0.99 ± 0.0002, dice ratio was 0.85 ± 0.08
	[35]	3D-UNet CNN	For metastasis segmentation, a median Dice score of 0.75 with high correlations between manually segmented and projected volumes was achieved.
	[36]	SVM	Improved mean AUC score from 0.53 to 0.74.
	[20]	DeepMedic	Mean AUC score improvement from 0.53 to 0.74 in internal cross-validation.
	[37]	Multi-scale cascaded CNN using 3D-enhanced T1-weighted MR images.	Demonstrated robustness across internal and external datasets.
	[38]	PCA, LR, SVM, RFC models	RFC model with multi-class features illustrated high efficiency with average F1 scores = 0.98.
	[39]	InceptionResNetV2 network, recurrent or transformer network, prediction difference analysis	Insightful outcome prediction with attention to spatial dependencies between MRI slices
	[20]	3D CNN based on DeepMedic.	Automated segmentations showed good volumetric correlation with manual segmentations.
	[40]	Deep Neural Network Ensemble learning model	Models trained on pooled data offer balanced predictive performance with ROC AUC=0.88±0.04.

3. METHODOLOGY

The proposed methodology for implementing and evaluating the U-Net model for BM segmentation involves several key steps. Initially, input images, including T1W1 (T1-weighted), T2W2 (T2-weighted), T1ce (T1-contrast enhanced), and FLAIR (Fluid-Attenuated Inversion Recovery) modalities, are gathered [41]. These images undergo data preprocessing, which includes resizing and normalization to ensure consistency and improve model performance. Subsequently, the dataset is split into training- 67%, testing-13%, and validation- 20% sets to facilitate robust model training and evaluation. The core of the approach is the use of the U-Net model with drop out layer, a prominent convolutional neural network architecture built for segmentation. The model has been trained using the training dataset, and its performance is measured using measures like accuracy, loss, Dice coefficient, and Intersection over Union (IOU). Validation is conducted concurrently to tune model parameters and prevent overfitting, using the same performance metrics. Post-training, the model undergoes rigorous testing to evaluate its final performance on unseen data, ensuring the metrics of accuracy, loss, Dice coefficient, and IOU are satisfactory. Finally, a comparative analysis is performed against other established models, including (CNN) Convolutional Neural Networks and (FCN) Fully Convolutional Networks.

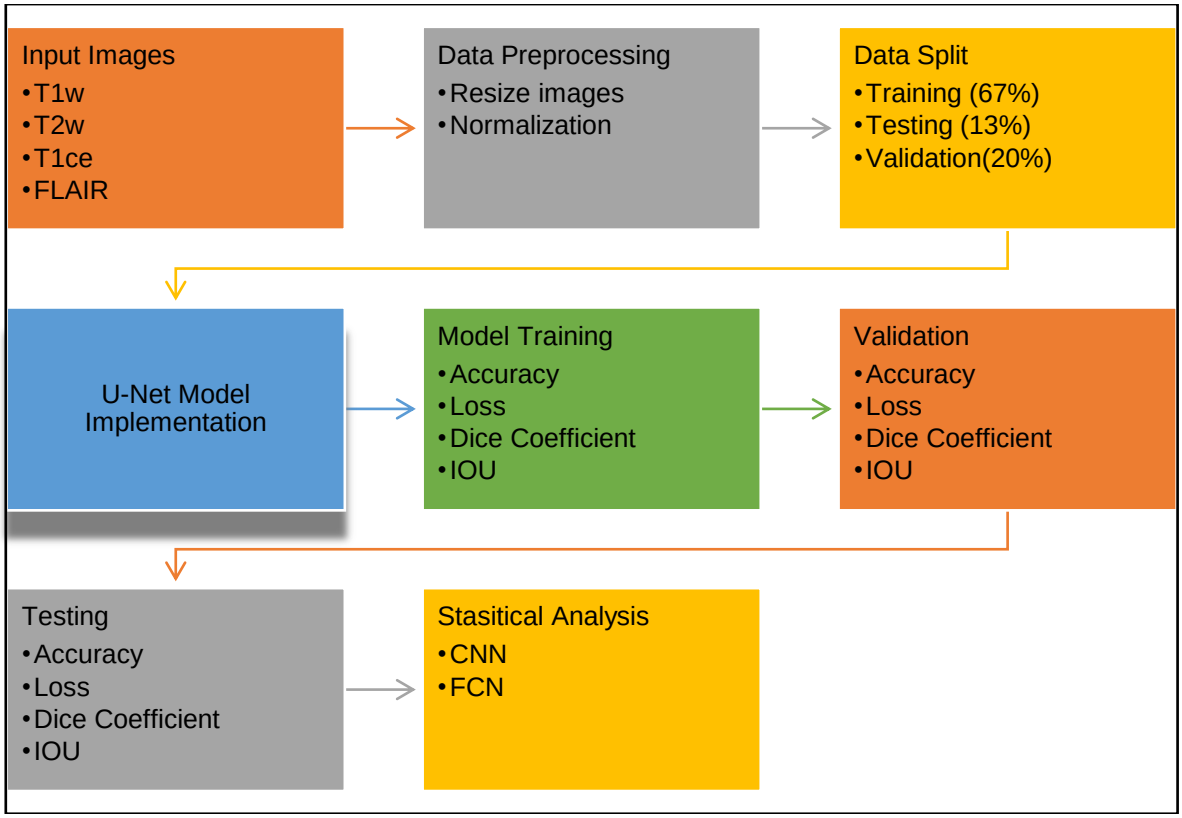

Fig 2. Proposed Research Methodology

3.1 Dataset

The model utilized an extensive neuroimaging dataset from the Brain Metastases Stereotactic Radiosurgery (UCSF-BMSR) MRI Dataset of the University of California, San Francisco[41]. It was collected from January 1, 2017, to February 29, 2020. Moreover, the code and data are publicly available and provide a platform that would encourage further research and development into the field of medical imaging and treatment related to brain metastasis. The dataset shall foster further development of the detection and segmentation of small brain metastases, since most of the public datasets available are focused on gliomas. This dataset contains 560 multimodal brain MR images from the records of 412 patients before and after undergoing Gamma Knife radiosurgery, with expert annotations for 5136 brain metastases; there are two different sets of annotations in 99 cases**.**

In proposed model, four essential imaging modalities for brain metastasis detection have been utilized i.e. T1-weighted (T1W1), T2-weighted (T2W1), Contrast-Enhanced T1-weighted (T1CE), and FLAIR (Fluid-Attenuated Inversion Recovery). These modalities have been selected due to their apparent ability to offer thorough anatomical insights pertinent to brain metastasis. In addition, the mask image is generated to highlight specific areas of interest (ROIs) in MRI images, such as tumours. The sample images have been shown in Fig 3.

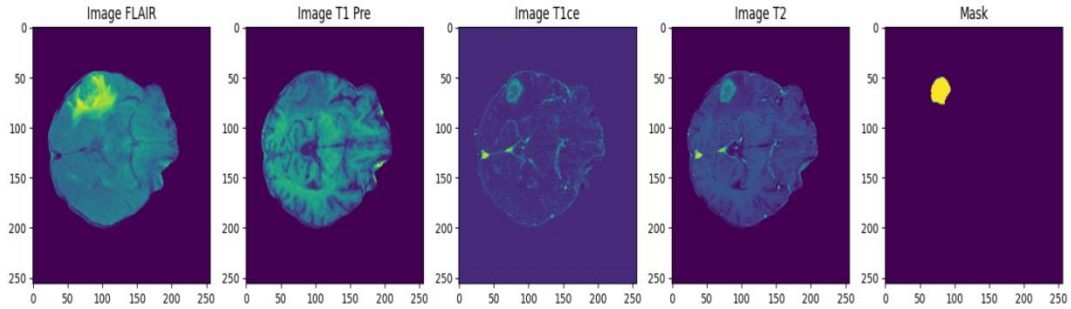

Fig 3. Sample Images

T1-weighted imaging shown as Image T1 Pre is essential in the assessment of metastatic brain lesions and blood-brain barrier breakdown, showing an MRI response to treatment by changes in size and

enhancement patterns of metastases. Similarly, T2-weighted imaging illustrated as Image T2 is essential for detecting brain metastases and associated edema, offering high tissue contrast to assess lesion size, impact, and additional metastases. T1 contrast-enhanced (Image T1ce) image acquisition is very important in the diagnosis, characterization, and treatment planning of brain metastases, for it increased lesion conspicuity and allows assessment of the integrity of the blood–brain barrier. Likewise, FLAIR imaging typically enhances the detection of brain metastases by suppressing CSF signals and improving contrast for the identification of lesions with a vasogenic edema. Masks are necessary in brain metastasis imaging to train machine learning models such as U-Net, which learn to anticipate these regions in new pictures. They are also used for quantitative analysis, such as determining tumour size and volume, and play an important role in treatment planning by defining tumour boundaries to guarantee exact targeting during therapies such as radiation or surgery [42].

The primary cancer sites mentioned in the dataset are lung cancer, breast cancer, melanoma and the pie chart for this distribution is demonstrated in Fig 4. below. The pie chart illustrates the distribution of primary cancer types among a given population. The largest segment represents lung cancer, which accounts for 39.0% of the cases. Breast cancer follows with a significant portion of 24.5%. Melanoma constitutes 16.3% of the cases, indicating its notable presence in the population. Renal cancer is less prevalent, making up 4.3% of the total cases. The remaining 15.8% are categorized under 'Others,' encompassing various fewer common types of primary cancers such as Esophogeal, Thyroid, GU Urothelial, Neuroendocrine etc.

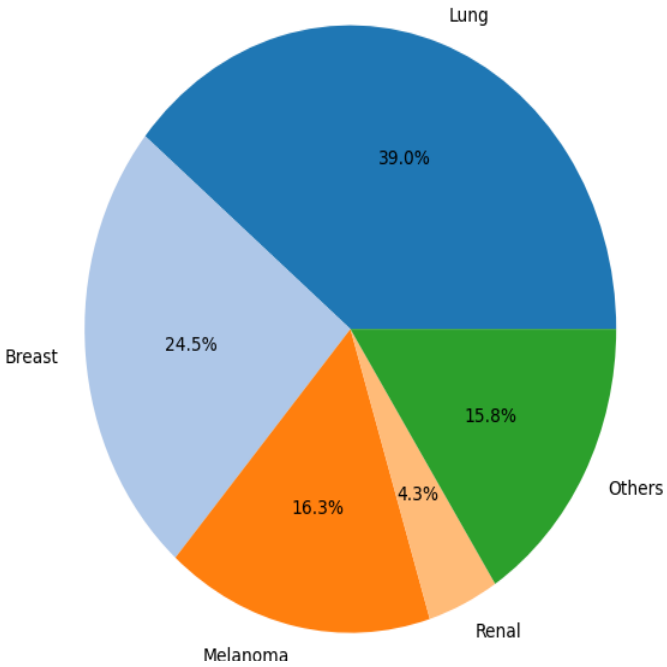

Fig 4. Primary Cancer Types

3.1.1 Data Preprocessing

The data preprocessing pipeline ensure the homogeneity and suitability of the dataset for effective model training. It includes several subprocesses such as resizing, standardization, normalization, and scaling so that the images are consistent in dimensions and pixel values. Resizing standardizes the image dimensions, while normalization scales the pixel values to a range of [0, 1], stabilizing the training process.

Resizing was done to 256x256 pixels, with all images normalized to avoid differences in scaling and minimize computational overhead. Intensities are normalized across modalities for better learning. Pre-processed FLAIR MRI test images, as shown in Figure 5, include the three standard orthogonal views with crosshairs for localization and colorization to enable the identification of features more easily.

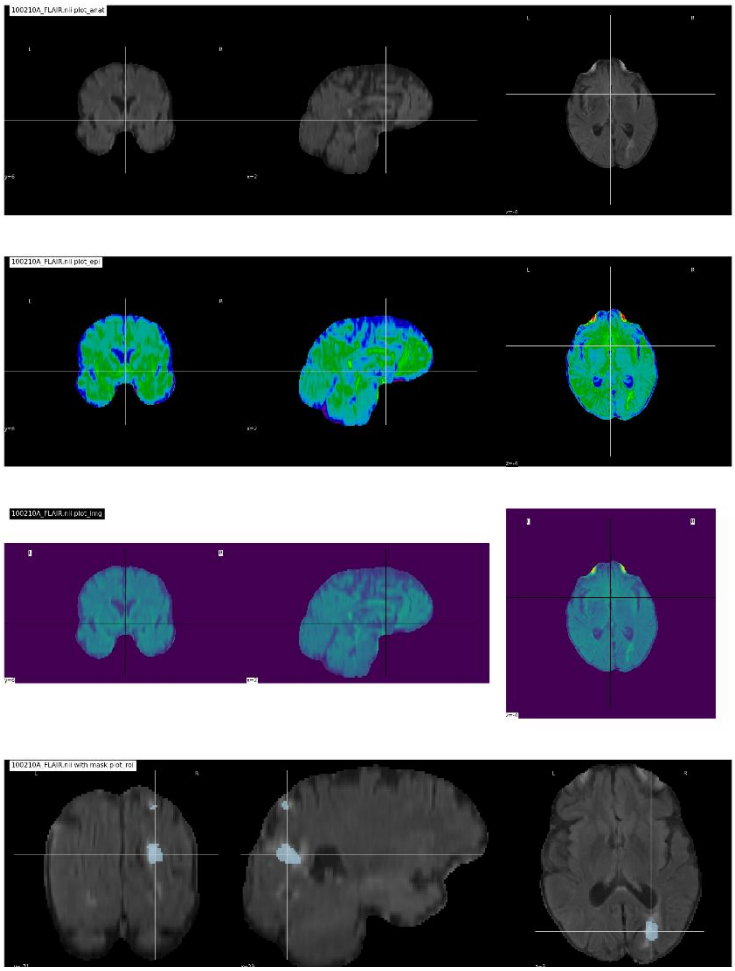

Fig 5. Pre-processed FLAIR MRI image

3.1.2 Data Split

Data splitting is a fundamental step in preparing datasets for deep learning, ensuring that models are trained, validated, and tested effectively. The dataset was rigorously separated into training (n=280), validation(n=83), and test (n=50) sets and demonstrated in Fig 6. to ensure a balanced distribution of samples across all classes while also preserving representative subsets for robust model training and evaluation.

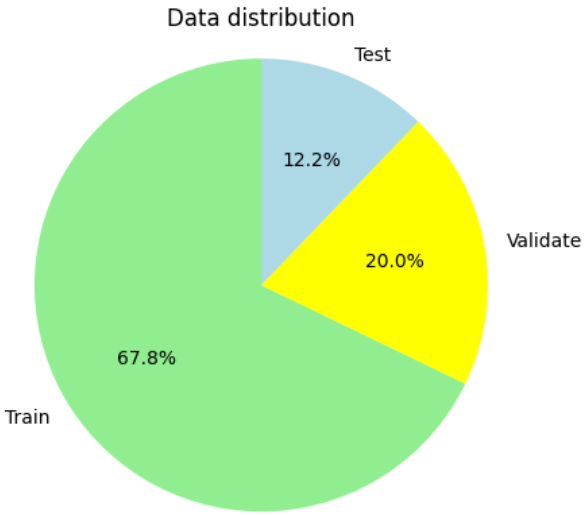

Fig 6. Data Distribution

6.4 U-Net Architecture

The deep learning model architecture for automated segmentation of brain metastases on MRI scans utilizes the U-Net architecture [35] with a dropout mechanism shown in Fig 7, a well-established framework for semantic segmentation tasks has been built using Python simulation environment.

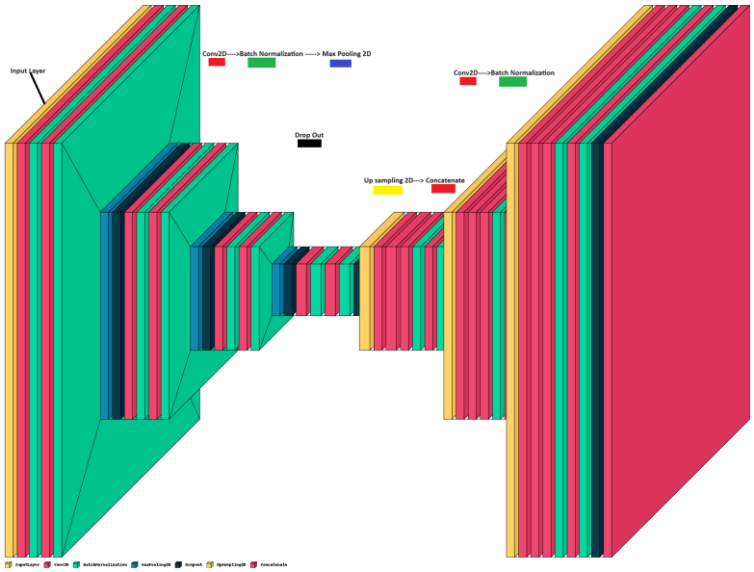

Fig 7. U-Net Model Architecture

This simulation environment for the segmentation of brain metastases contains all robust Python libraries. It includes TensorFlow for model construction, OpenCV and Skimage for image processing, and nibabel and nilearn for handling neuroimaging data. Moreover, it uses Pandas, NumPy, Matplotlib, and Seaborn for data manipulation and visualization, nlplt for plotting neuroimaging data, and pydot for graph visualization. It hence makes a whole pipeline from data preprocessing to model testing and visualization.
The U-Net is a convolutional neural network designed for biomedical image segmentation which consists of two parts: the contraction path (encoder) and the expansion path (decoder).
An encoder which is also known as the contraction path in the U-Net, is a critical part that goes towards reducing spatial dimensions by increasing feature maps. This path is crucial for capturing and compressing the important features of the input image, which is useful in, say, accurate segmentation functions, such as brain metastases identification in MRI scans. The contraction path consists of the first-level Conv2D, Batch Normalization, and Max Pooling 2D layers. The Conv2D layers are going to extract characteristics applying several filters to capture edge, textual, and form findings within the MRI images. After the Conv2D layers, Batch Normalization is applied to standardize and speed up the training process by normalizing the output of each convolutional layer. Finally, the Max Pooling 2D layers decrease the spatial dimensions of feature maps, keeping the most relevant features available with reduced computation. Together, these components ensure that the encoder effectively compresses the input data, enabling the model to focus on the most critical facets for segmentation.
The other important component of U-Net architecture is a decoder, also known as the expansion path, which reconstructs the spatial dimensions of feature maps compressed during the contraction phase. Such a path up samples the reduced feature maps back to the size of the original input image and produces detailed accurate segmentation maps. These make up the decoder, which consists of Up-Sampling 2D layers that increase the spatial dimensions of the feature maps, hence reversing the effects of the pooling operations in the encoder. After that, Conv2D layers are applied to refine the up-sampled feature maps so that the segmentation boundaries will be sharpened and the accuracy of the predictions increased. The decoder in the U-Net is also specialized by using Concatenate layers. It concatenates up-sampled feature maps with corresponding high-resolution feature maps previously obtained from the encoder to help the model retain relevant contextual information but at improved accuracy and higher resolution of the segmentation output. It ensures the U-Net model can produce accurate and detailed segmentation maps. Clinically, these are necessary for applications like brain metastasis detection and treatment planning.
Adam optimizer with a learning rate of 0.001 is used during training, and the callbacks used make sure efficient learning and adaptation to the intricacies of the task through learning rate adjustment, early stopping, and logging.

6.4.1 ALGORITHM: ALGORITHM TO DETECT SEGMENTED REGIONS INDICATING BRAIN METASTASES		
	Input: MRI images of the brain I ∈ R^ (H × W × C)	
	Output: Segmented regions indicating brain metastases	
1	Preprocess Data ←Normalize MRI images:	
		$\mathbf{I_{norm}} = \frac{(\mathbf{I} - \boldsymbol{\mu})}{\boldsymbol{\sigma}}$
2	Split data into training and validation sets.	
3	Train the model on the training set and validate on the validation set.	
	Notation: **I** = input image **Ci**= number of filters in the i-th layer **W**= weights of the convolutional filters **b** = biases **ReLU**= Rectified Linear Unit activation function **σ** =sigmoid activation function **BN** = Batch Normalization **Dropout(p)** = Drop out with probability **p** **MaxPool**= Max Pooling Operation **UpSample**= Up sampling operation ⊕ = Concatenation Operation	
4	Initialize U-Net Model ← **INPUT_LAYER (I) = I** ∈ $\mathbb{R}^{\mathbf{H*W*C}}$ **H** is the height, **W** is the width, and **C** is the number of channels.	
5	Contraction Path (Encoder)← for each level **l** ∈**{1, 2, 3, 4}**:	
		Apply Conv2D: $\mathbf{C1_l} = \mathbf{ReLU}(\mathbf{W_{1l}} * \mathbf{I} + \mathbf{b_{1l}})$
		Apply Batch Normalization: $\mathbf{BN1_l} = \mathbf{BN}(\mathbf{C1_l})$
		Apply Second Conv2D: $\mathbf{C2_l} = \mathbf{ReLU}(\mathbf{W})$
		Apply Batch Normalization: $\mathbf{BN2_l} = \mathbf{BN}(\mathbf{C2_l})$
		Apply Max Pooling: $\mathbf{P_l} = \mathbf{MaxPool}(\mathbf{BN2_l})$
		Apply Dropout: $\mathbf{D_l} = \mathbf{Dropout}(\mathbf{p})(\mathbf{P_l})$
6	Bottleneck← At the deepest layer of the U-Net	
		Apply Conv2D:$\mathbf{C5_1} = \mathbf{ReLU}(\mathbf{W_{5_1}} * \mathbf{D_4} + \mathbf{b_{5_1}})$
		Apply Batch Normalization: $\mathbf{BN5_1} = \mathbf{BN}(\mathbf{C5_1})$
		Apply Second Conv2D:$\mathbf{C5_2} = \mathbf{ReLU}(\mathbf{W_{5_2}} * \mathbf{BN5_1} + \mathbf{b_{5_2}})$
		Apply Batch Normalization:$\mathbf{BN5_2} = \mathbf{BN}(\mathbf{C5_2})$
7	Expansion Path (Decoder) ← for each level **l** in **{4, 3, 2, 1}**:	
		Apply Up Sampling:$\mathbf{U_l} = \mathbf{UpSample}(\mathbf{BN5_2})$
		Concatenate with the corresponding contraction path layer: $\mathbf{C_l} = \mathbf{U_l} \oplus \mathbf{D_{l-1}}$
		Apply Conv 2D: $\mathbf{E1_l} = \mathbf{ReLU}(\mathbf{W_{1_l}} * \mathbf{C_l} + \mathbf{b_{1_l}})$
		Apply Batch Normalization**:** $\mathbf{EBN1_l} = \mathbf{BN}(\mathbf{E1_l})$
		Apply Second Conv2D**:** $\mathbf{E2_l} = \mathbf{ReLU}(\mathbf{W_{2_l}} * \mathbf{EBN1_l} + \mathbf{b_{2_l}})$
		Apply Batch Normalization: $\mathbf{EBN2_l} = \mathbf{BN}(\mathbf{E2_l})$
8	Output Layer	
		Apply Conv 2D: $\mathbf{O} = \boldsymbol{\sigma}(\mathbf{W_{out}} * \mathbf{EBN2_1} + \mathbf{b_{out}})$
9	Compile Model	
		Loss Function: Binary Cross-Entropy $\mathbf{Loss} = -\frac{\mathbf{1}}{\mathbf{N}}\sum_{\mathbf{i=1}}^{\mathbf{N}}[\mathbf{y_i}\,\mathbf{log}(\hat{\mathbf{y}}_\mathbf{i}) + (\mathbf{1} - \mathbf{y_i})\mathbf{log}(\mathbf{1} - \hat{\mathbf{y}}_\mathbf{i})]$
		Optimizer: Adam
10	Evaluate Model:	
		$\mathbf{Accuracy} = \frac{\mathbf{Number\ of\ Correct\ Predictions}}{\mathbf{Total\ number\ of\ Predictions}}$ $\mathbf{Dice} = \frac{\mathbf{2} * \lvert\mathbf{X_{pred}} \cap \mathbf{X_{true}}\rvert}{\lvert\mathbf{X_{pred}}\rvert + \lvert\mathbf{X_{true}}\rvert}$
		$\mathbf{Loss} = \mathbf{Categorical\ Cross} - \mathbf{Entropy}$
		$\mathbf{IoU} = \frac{\lvert\mathbf{X_{pred}} \cap \mathbf{X_{true}}\rvert}{\lvert\mathbf{X_{pred}} \cup \mathbf{X_{true}}\rvert}$

11	Predict segmentation masks for new MRI images using the trained model.
12	End

6.5 Results and Analysis

The U-Net model established for brain metastases segmentation shows excellent performance in overall accurately tumor regions delineation, which is particularly important to early detection. Early diagnosis is paramount to mitigating the neurocognitive sequelae of brain metastasis and their treatments. The training procedure involves data handling through a custom-made data generator to efficiently deal with large datasets without memory overflow. It is trained for several epochs, aided by callbacks, until optimal learning rate adjustment, early stopping, and logging. This iterative process helps the model learn and adapt to the complexities of brain metastases segmentation. Through extensive training and validation, the model has not only achieved remarkable accuracy but also shown its ability to capture the nuanced boundaries of various tumor classes. The findings suggest that the proposed model is not only highly accurate in achieving good overall performance, but also performs well on segmenting certain key regions such as enhancing region and edema or core/nonenhancing necrotic areas which have a direct impact on clinical management of patient to help improve outcomes. The following sections provide a comprehensive evaluation of the model's capabilities, combining both qualitative and quantitative assessments.

6.5.1 Visual Analysis of Segmentation Performance

To evaluate the model's segmentation capabilities, the visual output of the U-Net model has been analyzed by comparing the predicted segmentation maps with the ground truth annotations. The close alignment between the predicted segmentations and the ground truth highlights the model's robustness in capturing intricate details, offering a clear visual validation of its effectiveness. The segmentation images shown in Fig 8. illustrate the U-Net model's performance in identifying and segmenting different regions of brain metastases on FLAIR MRI scans.

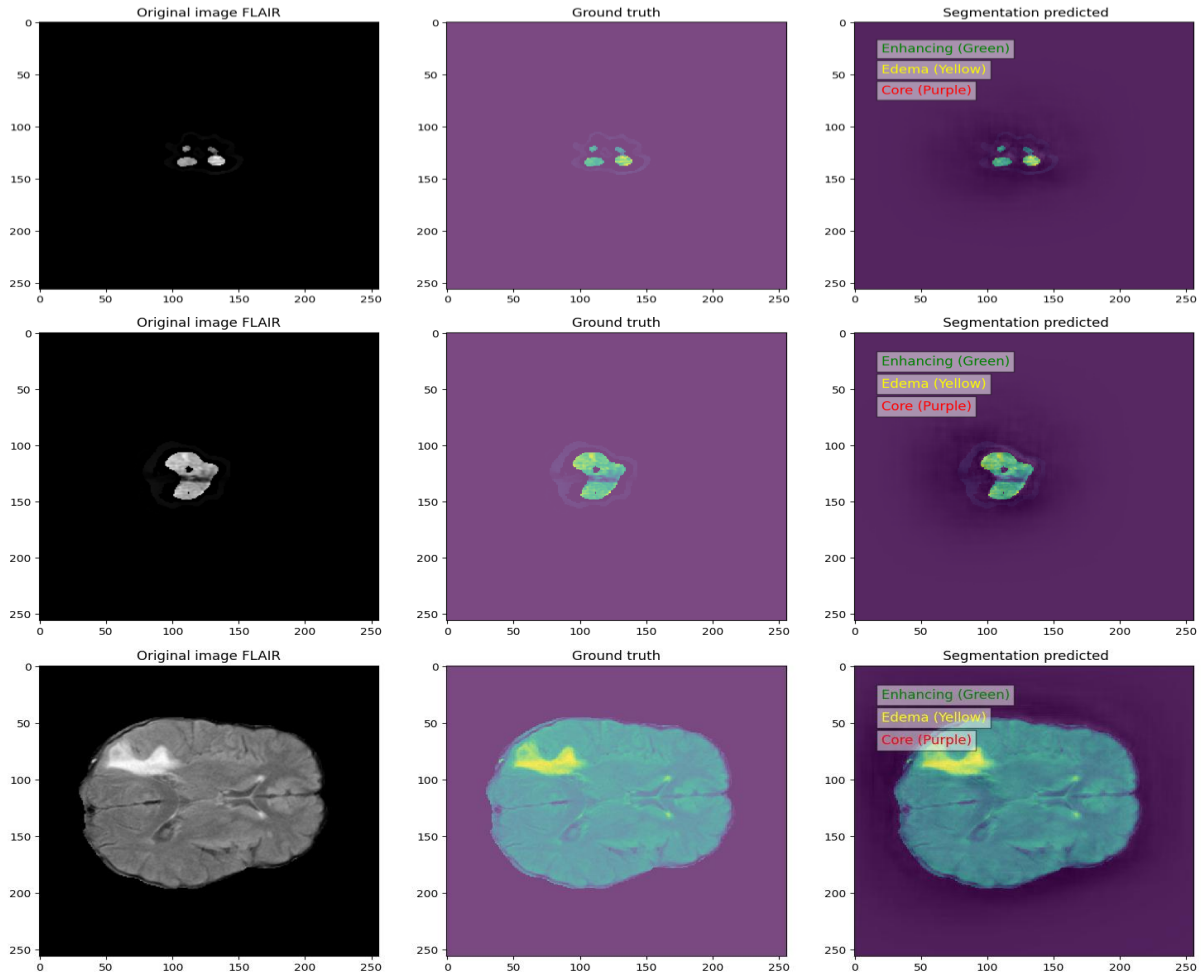

Fig 8. Predicted Segmentation Classes

The three panels in Figure 8. are the original FLAIR scan, the ground truth segmentation, and the predicted segmentation. The FLAIR scan shows a visualization of abnormality in the brain, and the enhancing component of the tumor appears as a bright region. The ground truth was manually annotated by experts to demarcate the regions of the tumor: enhancing tissue is green, edema yellow, and the necrotic core purple. It predicts the segmentation of these regions, showing great alignment with the ground truth, depicted in the third panel. This kind of model is very useful in the early detection of brain metastasis since it identifies and segments different parts of the tumor very well. Even segmentation would lead to an early prediction of BM, which would help in the timely treatment that may mitigate neurocognitive decline caused by the tumor progression.

6.5.2 Evaluation Metrics

To comprehensively assess the model's segmentation performance, a suite of metrics was employed, including accuracy, mean Intersection over Union (IoU), and class-specific Dice coefficients. These metrics provided a detailed understanding of the model's ability to accurately delineate various tumor regions.

- Average Loss: A remarkably low average loss of 0.0052 indicates the model's effective learning during training.
- Overall Accuracy: With an impressive accuracy of 99.75%, the model demonstrated its proficiency in distinguishing tumor and non-tumor regions.
- Average Intersection over Union (IoU): An average IoU of 96.81% highlights the model's precise segmentation capabilities.
- Average Dice Coefficient: A Dice coefficient of 64.49% underscores the model's ability to capture intricate tumor boundaries.
- Average Precision: High precision of 99.75% indicates minimal false positives.
- Average Sensitivity: A sensitivity of 99.70% demonstrates the model's effectiveness in capturing true positives.
- Average Specificity: A high specificity of 99.90% highlights the model's ability to accurately identify true negatives.

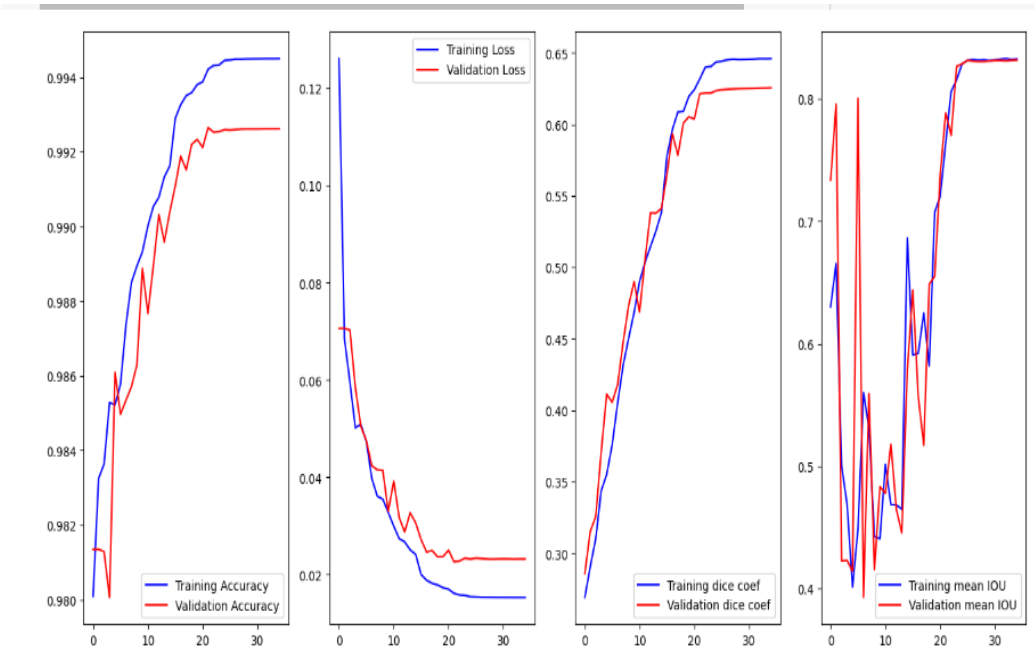

Fig 9. Evaluation Metric Curves using U-Net CNN

This performance is apparent in the training and validation curves: although the accuracy and dice coefficient in both the training and validation sets increase as expected, the loss curves for both will show a downward trend, thus indicating the model is minimizing errors. Although the validation metrics look like they follow some small trends, especially in the very early epochs, they generalize quite well: there is barely any overfitting in this model. The consistent improvement of IoU explains the model's ability for correct tumor areas segmentation of brain metastases while false positives are kept minimum.

6. Comparative Analysis

The proposed methodology is compared against existing state-of-the-art segmentation models-namely, CNN, Convolutional Network, and FCN, Fully Convolutional Network-on the same dataset. Table 4. shows the superiority of the proposed U-Net CNN model compared to the results of both traditional CNNs and to a fully convolutional neural network, FCN. For correctness, the U-Net CNN is top of all other models scored on 0.9975 for the training dataset and 0.993 for the validation dataset. Furthermore, the loss values for the U-Net CNN are also the lowest among them: 0.0052 for training and 0.0025 for validation, meaning that the values it predicted are the closest to the real ones. Hence, the U-Net CNN model again performed significantly better than all the CNN models in Dice Coefficient, where the training score was 0.6449 and validation was even better, with 0.631. It means that it is an overlap measure between the predicted and true regions and is an improved way of learning to address imbalanced data. In a similar manner, the High IOU-Maintained U-Net CNN had the highest IOU values up to 0.9681 for the training and the same value for the validation, therefore proving its efficiency in the correct segmentation of data.

Table 4. Comparative Performance Metrics of U-Net CNN, Traditional CNN, and FCN

Model		Accuracy	Loss	Dice Coefficient	IOU
U-Net CNN	Training	0.9975	0.0052	0.6449	0.9681
	Validation	0.993	0.0025	0.631	0.9681
Traditional CNN	Training	0.9676	0.038	0.388	0.707
	Validation	0.9778	0.036	0.372	0.705
FCN	Training	0.9699	0.035	0.44	0.6999
	Validation	0.97	0.32	0.423	0.703

The Traditional CNN and FCN models show lower accuracy, higher loss, and substantially lower Dice Coefficient and IOU values, particularly highlighting the Traditional CNN's weaker performance in segmentation tasks compared to the more specialized U-Net architecture.

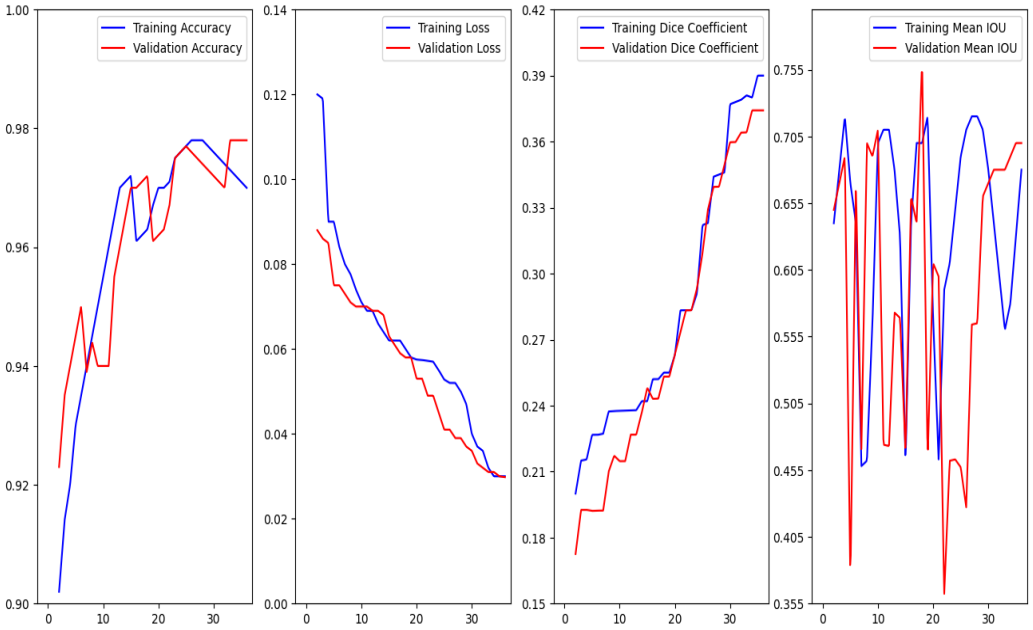

Fig 10. Evaluation Metric Curves using traditional CNN

The traditional CNN model shown in Fig 10. achieved an accuracy of 96.76% with a loss of 0.038, a Dice Coefficient of 38.8%, and an Intersection over Union (IOU) of 70.7%. During validation, the model maintained a high accuracy of 97.78%, with a slightly reduced loss of 0.036. The Dice Coefficient and IOU during validation were 37.2% and 70.5%, respectively. Similarly, Fig 11. demonstrated the performance metric curves for Fully Convolutional Network (FCN) that achieved an accuracy of 96.99%, with a loss of 0.035, a Dice Coefficient of 44%, and an Intersection over Union (IOU) of 69.99%. In the validation phase, the model maintained a high accuracy of 97.00%, with a slightly higher loss of 0.32. The Dice Coefficient and IOU during validation were 42.3% and 70.3%, respectively.

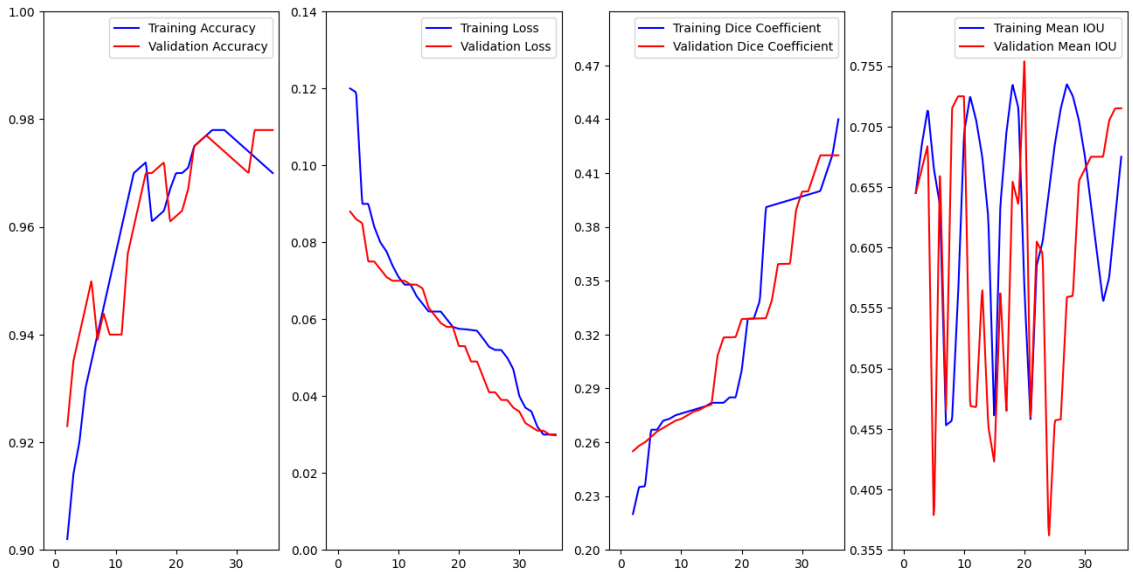

Fig 11. Evaluation Metric Curves using FCN

The performance metric curves, illustrates that the U-Net CNN model shown in Fig 9. demonstrates superior performance compared to both the Traditional CNN and the Fully Convolutional Network (FCN). The U-Net CNN consistently achieves higher accuracy and Dice Coefficient values, as well as lower loss values, indicating more precise and reliable predictions. Additionally, the Intersection over Union (IOU) scores for the U-Net CNN are notably higher, further highlighting its effectiveness in segmentation tasks. The performance curves visually reinforce these findings, showing a clear distinction in the performance trends of the U-Net CNN over the other models.

7. CONCLUSION

The results demonstrate a detailed methodology of the automated segmentation of brain metastases using the U-Net CNN model, which surpassed the Traditional CNN and FCN models. The best metrics achieved by the U-Net CNN model are impressive, sometimes achieving even the lowest loss value with the highest Dice Coefficient and IOU metrics, in comparisons conducted between the two datasets, for both the training and validation set. The performance curves further validate the results, which have illustrated consistency and reliability of the model for segmenting brain metastases. U-Net CNN could be capable of handling imbalanced datasets, and its higher degree of precision in evaluating the effectiveness of the treatment continues to outline this potential for real-world applications in a clinical environment. Moreover, the methodology embraced would determine the generalizability and suitability of the model for use on a wide range of datasets. The paper makes a rigorous comparative study between U-Net CNN and Traditional CNN and FCN models, which shines light on the superior capabilities of the former. The technique used here might be found useful in the arsenal for diagnosing brain metastases.

In conclusion, the U-Net CNN model offers a significant advancement in the automated detection and segmentation of brain metastases, contributing to the enhancement of diagnostic tools and ultimately improving patient outcomes through timely and accurate decision-making. Future research should focus on further refining the model, exploring additional imaging modalities, and validating its performance in larger, more diverse patient cohorts to ensure its widespread clinical adoption.

REFERENCES

[1] H.-S. Gwak, “Molecular Biology of Brain Metastases,” Brain Tumor Res Treat, vol. 11, no. 1, p. 8, 2023, doi: 10.14791/btrt.2022.0045.

[2] M. Łazarczyk et al., “The Journey of Cancer Cells to the Brain: Challenges and Opportunities,” Feb. 01, 2023, Multidisciplinary Digital Publishing Institute (MDPI). doi: 10.3390/ijms24043854.

[3] B. K. Campbell, Z. Gao, N. M. Corcoran, S. S. Stylli, and C. M. Hovens, “Molecular Mechanisms Driving the Formation of Brain Metastases,” Oct. 01, 2022, MDPI. doi: 10.3390/cancers14194963.

[4] A. M. Eraky, “Advances in Brain Metastases Diagnosis: Non-coding RNAs As Potential Biomarkers,” Cureus, Mar. 2023, doi: 10.7759/cureus.36337.

[5] L. Jiang and C. Zhang, "Complete response with combined therapy in a patient with brain metastasis from nasopharyngeal carcinoma: case report and literature review," Journal of International Medical Research, vol. 51, no. 1, Jan. 2023, doi: 10.1177/03000605221147187.
[6] "2017_Cognitive Impairment Associated with Cancer".
[7] A. Gerstenecker et al., "Cognition in patients with newly diagnosed brain metastasis: Profiles and implications," J Neurooncol, vol. 120, no. 1, pp. 179–185, Sep. 2014, doi: 10.1007/s11060-014-1543-x.
[8] T. A. Ahles and J. C. Root, "Cognitive Effects of Cancer and Cancer Treatments," May 07, 2018, Annual Reviews Inc. doi: 10.1146/annurev-clinpsy-050817-084903.
[9] W. C. M. Schimmel, K. Gehring, D. B. P. Eekers, P. E. J. Hanssens, and M. M. Sitskoorn, "Cognitive effects of stereotactic radiosurgery in adult patients with brain metastases: A systematic review," Oct. 01, 2018, Elsevier Inc. doi: 10.1016/j.adro.2018.06.003.
[10] A. W. Moawad et al., "Link 18, †, ‡ , Nourel hoda Tahon 19."
[11] "Automated segmentation of brain metastases in T1-weighted contrast-enhanced MR images pre and post Stereotactic Radiosurgery", doi: 10.1101/2023.07.07.23292387.
[12] I. Grazzini, D. Venezia, D. Del Roscio, I. Chiarotti, M. A. Mazzei, and A. Cerase, "Morphological and Functional Neuroradiology of Brain Metastases," Seminars in Ultrasound, CT and MRI, vol. 44, no. 3, pp. 170–193, 2023, doi: https://doi.org/10.1053/j.sult.2023.03.004.
[13] M. N. Bongers, G. Bier, C. Schabel, J. Fritz, and M. Horger, "Detectability of brain metastases by using frequency-selective nonlinear blending in contrast-enhanced computed tomography," Invest Radiol, vol. 54, no. 2, pp. 98–102, Feb. 2019, doi: 10.1097/RLI.0000000000000514.
[14] S. H. A. E. Derks, A. A. M. van der Veldt, and M. Smits, "Brain metastases: the role of clinical imaging," 2022, British Institute of Radiology. doi: 10.1259/BJR.20210944.
[15] L. Urso et al., "The Role of Molecular Imaging in Patients with Brain Metastases: A Literature Review," Apr. 01, 2023, Multidisciplinary Digital Publishing Institute (MDPI). doi: 10.3390/cancers15072184.
[16] N. P. Dang, G. Noid, Y. Liang, J. A. Bovi, M. Bhalla, and A. Li, "Automated Brain Metastasis Detection and Segmentation Using Deep-Learning Method," International Journal of Radiation Oncology*Biology*Physics, vol. 114, no. 3, p. e50, Nov. 2022, doi: 10.1016/j.ijrobp.2022.07.784.
[17] A. Sanchez-Aguilera et al., "Machine learning identifies experimental brain metastasis subtypes based on their influence on neural circuits," Cancer Cell, vol. 41, no. 9, pp. 1637-1649.e11, Sep. 2023, doi: 10.1016/j.ccell.2023.07.010.
[18] S. R. Sowrirajan and S. Balasubramanian, "Brain Tumor Classification Using Machine Learning and Deep Learning Algorithms," International Journal of Electrical and Electronics Research, vol. 10, no. 4, pp. 999–1004, 2022, doi: 10.37391/ijeer.100441.
[19] V. Verma, A. Aggarwal, and T. Kumar, "Machine and Deep Learning Approaches For Brain Tumor Identification: Technologies, Applications, and Future Directions," in Proceedings of International Conference on Computational Intelligence and Sustainable Engineering Solution, CISES 2023, Institute of Electrical and Electronics Engineers Inc., 2023, pp. 392–399. doi: 10.1109/CISES58720.2023.10183492.
[20] S. T. Jünger et al., "Fully Automated MR Detection and Segmentation of Brain Metastases in Non-small Cell Lung Cancer Using Deep Learning," Journal of Magnetic Resonance Imaging, vol. 54, no. 5, pp. 1608–1622, Nov. 2021, doi: 10.1002/jmri.27741.
[21] S. K. Yoo, T. H. Kim, H. J. Kim, H. I. Yoon, and J. S. Kim, "Deep Learning-Based Automatic Detection and Segmentation of Brain Metastases for Stereotactic Ablative Radiotherapy Using Black-Blood Magnetic Resonance Imaging," International Journal of Radiation Oncology*Biology*Physics, vol. 114, no. 3, p. e558, Nov. 2022, doi: 10.1016/j.ijrobp.2022.07.2196.
[22] E. Grøvik et al., "Handling missing MRI sequences in deep learning segmentation of brain metastases: a multicenter study," NPJ Digit Med, vol. 4, no. 1, Dec. 2021, doi: 10.1038/s41746-021-00398-4.
[23] Z. Qian et al., "Differentiation of glioblastoma from solitary brain metastases using radiomic machine-learning classifiers," Cancer Lett, vol. 451, pp. 128–135, Jun. 2019, doi: 10.1016/j.canlet.2019.02.054.
[24] N. C. Swinburne et al., "Machine learning for semiautomated classification of glioblastoma, brain metastasis and central nervous system lymphoma using magnetic resonance advanced imaging," Ann Transl Med, vol. 7, no. 11, pp. 232–232, Jun. 2019, doi: 10.21037/atm.2018.08.05.
[25] S. Bae et al., "Robust performance of deep learning for distinguishing glioblastoma from single brain metastasis using radiomic features: model development and validation," Sci Rep, vol. 10, no. 1, Dec. 2020, doi: 10.1038/s41598-020-68980-6.

[26] Z. Liu et al., "Handcrafted and Deep Learning-Based Radiomic Models Can Distinguish GBM from Brain Metastasis," J Oncol, vol. 2021, 2021, doi: 10.1155/2021/5518717.
[27] A. Stadlbauer et al., "Differentiation of Glioblastoma and Brain Metastases by MRI-Based Oxygen Metabolomic Radiomics and Deep Learning," Metabolites, vol. 12, no. 12, Dec. 2022, doi: 10.3390/metabo12121264.
[28] S. J. Müller, E. Khadhraoui, M. Ernst, V. Rohde, B. Schatlo, and V. Malinova, "Differentiation of multiple brain metastases and glioblastoma with multiple foci using MRI criteria," BMC Med Imaging, vol. 24, no. 1, Dec. 2024, doi: 10.1186/s12880-023-01183-3.
[29] A. Fauzi, Y. Yueniwati, A. Naba, and R. F. Rahayu, "Performance of deep learning in classifying malignant primary and metastatic brain tumors using different MRI sequences: A medical analysis study," J Xray Sci Technol, vol. 31, no. 5, pp. 893–914, 2023, doi: 10.3233/XST-230046.
[30] A. de Causans et al., "Development of a Machine Learning Classifier Based on Radiomic Features Extracted From Post-Contrast 3D T1-Weighted MR Images to Distinguish Glioblastoma From Solitary Brain Metastasis," Front Oncol, vol. 11, Jul. 2021, doi: 10.3389/fonc.2021.638262.
[31] J. H. Oh, K. M. Lee, H. G. Kim, J. T. Yoon, and E. J. Kim, "Deep learning-based detection algorithm for brain metastases on black blood imaging," Sci Rep, vol. 12, no. 1, Dec. 2022, doi: 10.1038/s41598-022-23687-8.
[32] H. Jeong, J. E. Park, N. Y. Kim, S. K. Yoon, and H. S. Kim, "Deep learning-based detection and quantification of brain metastases on black-blood imaging can provide treatment suggestions: a clinical cohort study," Eur Radiol, 2023, doi: 10.1007/s00330-023-10120-5.
[33] J. Kottlors et al., "Contrast-enhanced black blood mri sequence is superior to conventional t1 sequence in automated detection of brain metastases by convolutional neural networks," Diagnostics, vol. 11, no. 6, Jun. 2021, doi: 10.3390/diagnostics11061016.
[34] J. Xue et al., "Deep learning-based detection and segmentation-assisted management of brain metastases," Neuro Oncol, vol. 22, no. 4, pp. 505–514, Apr. 2020, doi: 10.1093/neuonc/noz234.
[35] J. D. Rudie et al., "Three-dimensional u-net convolutional neural network for detection and segmentation of intracranial metastases," Radiol Artif Intell, vol. 3, no. 3, May 2021, doi: 10.1148/ryai.2021200204.
[36] P. Sommer et al., "Risk Classification of Brain Metastases via Radiomics, Delta-Radiomics and Machine Learning," Feb. 2023, [Online]. Available: http://arxiv.org/abs/2302.08802
[37] S. Yin et al., "Development and validation of a deep-learning model g p a multi-center multi-reader evaluation study," Neuro Oncol, vol. 24, no. 9, pp. 1559–1570, Sep. 2022, doi: 10.1093/neuonc/noac025.
[38] C. Cui et al., "Improving the Classification of PCNSL and Brain Metastases by Developing a Machine Learning Model Based on 18F-FDG PET," J Pers Med, vol. 13, no. 3, Mar. 2023, doi: 10.3390/jpm13030539.
[39] S. A. Jalalifar, H. Soliman, A. Sahgal, and A. Sadeghi-Naini, "Predicting the outcome of radiotherapy in brain metastasis by integrating the clinical and MRI-based deep learning features," Med Phys, vol. 49, no. 11, pp. 7167–7178, Nov. 2022, doi: 10.1002/mp.15814.
[40] J. Zhao et al., "A Radiogenomic Deep Ensemble Learning Model for Identifying Radionecrosis Following Brain Metastasis Stereotactic Radiosurgery (SRS)," 2024.
[41] J. D. Rudie et al., "The University of California San Francisco, Brain Metastases Stereotactic Radiosurgery (UCSF-BMSR) MRI Dataset."
[42] S. Das, N. S. Dey, and M. Mounika, "Automated Brain Tumor Segmentation in MRI : An Enhanced Mask Generation Approach," in 2023 7th International Conference on I-SMAC (IoT in Social, Mobile, Analytics and Cloud) (I-SMAC), 2023, pp. 891–897. doi: 10.1109/I-SMAC58438.2023.10290265.